Universiteit Leiden
The Netherlands

New chemical tools to illuminate N-acylphosphatidylethanolamine biosynthesis
Wendel, T.J.

Citation
Wendel, T. J. (2023, March 23). *New chemical tools to illuminate N-acylphosphatidylethanolamine biosynthesis*. Retrieved from https://hdl.handle.net/1887/3576707

7

Summary and future prospects

N-acylphosphatidylethanolamines (NAPEs) are a diverse family of lipids with multifaceted biological functions, but they are relatively underexplored.[1,2] Recently, Phospholipase A2 Group IV E (PLA2G4E) was shown to be capable of calcium-dependent production of NAPEs in cells.[3,4] PLA2G4E is a member of the PLA2G4 family, which consists of six serine hydrolases (PLA2G4A–F).[5] These enzymes are characterized by a Ser-Asp catalytic dyad and an N-terminal calcium-dependent lipid binding C2 domain.[5,6] PLA2G4E has an additional C-terminal polybasic stretch which is involved in its subcellular localization.[7] It was reported to be a principal *N*-acyltransferase that is able to synthesize NAPEs in a calcium-dependent fashion.[3] It is mainly expressed in brain, testes, heart and skeletal muscle, and expression levels were linked to Alzheimer's disease and panic disorder.[3,8,9] In addition, it appeared to be involved in recycling cargo from the clathrin-independent endocytic machinery back to the plasma membrane.[7] Whether NAPEs are involved in these functions is unclear.

No inhibitors of PLA2G4E have been published to date. PLA2G4E inhibitors would be instrumental in elucidating the physiological role of this enzyme in NAPE biology in an acute and time-dependent manner. Selective inhibitors are also required to establish the therapeutic potential of targeting PLA2G4E. Therefore, the overarching aim of this thesis was to develop cellular active inhibitors of PLA2G4E.

Chapter 1 gives a comprehensive overview of the current understanding of NAPE biology and PLA2G4E. NAPEs are glycerophospholipids with three fatty acyl groups. When these are embedded in lipid membranes, NAPEs may be involved in regulation of membrane dynamics, including membrane curvature, fusion and interactions with membrane-associated proteins.[10–14] NAPEs may also serve as signaling molecules. Hypophagic functions have been attributed to them, though it is disputed whether the effects reported are truly NAPE-specific.[15,16] Their levels are markedly increased in degenerating tissue, an effect observed in e.g. infarcted heart, ischemic brain and inflamed testes.[17–19] In addition, NAPE levels are elevated in models of neurodegeneration, and a protective role has been proposed in Parkinson's disease.[14,20–22] Furthermore, biosynthesis and metabolism of NAPEs plays an important role in the homeostasis of other structural and signaling lipids. They are produced from phosphatidylethanolamine (PE) and phosphatidylcholine (PC)[3,23], levels of which have also been linked to neurodegenerative diseases.[24–26] Four pathways for the metabolism of NAPEs to *N*-acylethanolamines (NAEs) have been reported, generating various classes of important metabolites, including phosphatidic acid (PA), lysophosphatidic acid (LPA) and free fatty acids (FFAs).[27] Depending on their structure, NAEs exert diverse signaling functionalities through the activation of various receptors, which leads to satietal, anti-inflammatory, analgesic, anti-addictive or anxiolytic effects, among others.[28–34] NAEs are metabolized by the enzyme fatty acid amide hydrolase (FAAH), terminating their biological actions.

In **Chapter 2**, the development of novel PLA2G4E inhibitors is reported. Previously, a competitive activity-based protein profiling (ABPP) assay was developed to measure the

activity of PLA2G4E.[35] Screening of a focused library of lipase inhibitors identified 1,2,4-triazole ureas as inhibitors of PLA2G4E. Compound **1** was selected as starting point for hit optimization, based on its potency, lipophilic efficiency (LipE) and ligand efficiency (LE) (Figure 7.1A). 26 analogs were synthesized and tested for inhibitory activity with the aim of deducing structure-activity relationships (SAR) and improving the potency. Increasing the distance between the phenyl in the amine group and the reactive urea and increasing steric bulk resulted in improved potency, leading to the identification of a 4-benzyl-piperidine group providing 10-fold potency improvement. *Ortho* and *meta* substitutions on this benzyl ring were tolerated, but *para* substitutions were preferred. 4-(4-Chloro-benzyl)piperidine-containing compound **WEN091** was identified as the most potent PLA2G4E inhibitor (pIC_{50} = 8.01 ± 0.02). **WEN091** demonstrated ~100-fold potency increase compared to **1** and improved LipE and LE (Figure 7.1A).
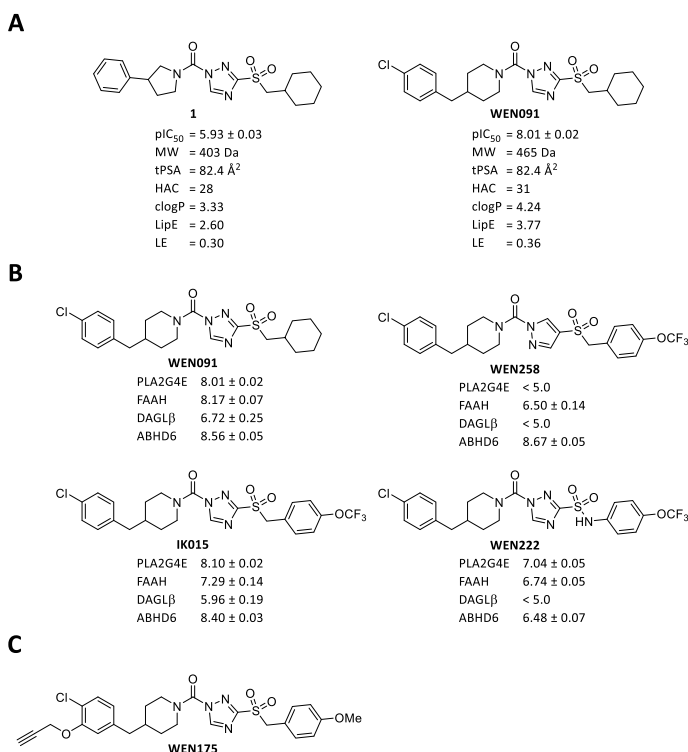
Figure 7.1. Structures and properties of PLA2G4E inhibitors 1–WEN175. A) Potency and physicochemical properties of hit **1** and inhibitor **WEN091**. Potency on PLA2G4E determined using gel-based ABPP on HEK293T overexpression lysate (pIC_{50} ± SEM, N ≥ 2). Molecular weight (MW) and topological polar surface area (tPSA) calculated using ChemDraw Professional 16.0; HAC = heavy atom count; Lipophilic efficiency LipE = pIC_{50} – clogP (DataWarrior 5.0.0); Ligand efficiency LE = $1.4pIC_{50}$/HAC. B) Inhibitory activity of inhibitors **WEN091–WEN258** (pIC_{50} ± SEM) determined using gel-based ABPP on overexpression lysate (PLA2G4E) or Neuro-2a cells (FAAH, DAGLβ, ABHD6) (N ≥ 2). C) Chemical structure of PLA2G4E probe **WEN175**.

WEN091 was further biochemically profiled in **Chapter 3**. The activity on PLA2G4E was tested in a natural substrate conversion assay based on liquid chromatography-mass spectrometry (LC-MS) analysis. **WEN091** dose-dependently inhibited the formation of NAPE from exogenous PC and PE in human and mouse PLA2G4E overexpression lysate as well as in mouse brain homogenate (pIC_{50} = 6.9–7.1). The compound was more than 20-fold selective over PLA2G4B–D and at least ten-fold over the calcium-independent NAPE biosynthetic enzymes phospholipase A/acyltransferase (PLAAT) 2–5. The compound was not active on NAPE phospholipase D (NAPE-PLD) or the cannabinoid ($CB_{1/2}$) receptors. ABPP profiling of its selectivity on mouse brain proteome and living cells showed inhibition of several serine hydrolases, such as ABHD6, DAGLα and FAAH. **WEN091**, but not its negative control analog **WEN258** (see below), reduced endogenous cellular levels of NAPEs, lyso-NAPEs and glycerophospho-palmitoylethanolamine. Both compounds showed cellular activity on FAAH, but only treatment with **WEN258** affected the NAE levels, suggesting that steady state NAE levels in these cells are controlled by PLA2G4E and FAAH. *N*-22:6 lyso-NAPE levels were not elevated in overexpressing cells, but were after treatment with **WEN091** or **WEN258**, leading to the hypothesis that these lipids are biosynthesized in a PLA2G4E and ABHD4-independent fashion. Both inhibitors lowered levels of the endocannabinoid 2-arachidonoylglycerol (2-AG), but only **WEN091** showed inhibition of its biosynthetic enzyme DAGLβ. This suggested ABHD6 might be responsible for tonic 2-AG production in these cells, which is in line with previous findings.[36] In conclusion, **WEN091** is a potent PLA2G4E inhibitor with selectivity for calcium-dependent NAPE biosynthesis *in vitro* that was able to reduce PLA2G4E-mediated NAPE production in Neuro-2a cells.

In **Chapter 4**, the SAR study of PLA2G4E inhibitors was expanded with 38 analogs of **WEN091** to improve its selectivity over FAAH. It was concluded that the sulfone was important for activity on PLA2G4E, but not on FAAH. Converting this to a sulfonamide decreased activity on both enzymes and led to lower selectivity. Bulky substituents on the triazolyl leaving group provided higher selectivity over FAAH, leading to the identification of 4-trifluoromethoxybenzyl-containing compound **IK015** as potent PLA2G4E inhibitor (pIC_{50} = 8.10 ± 0.02) with over 800-fold selectivity over FAAH *in vitro* (Figure 7.1B). Further investigation of the steric and electronic properties of this benzyl group did not improve the potency or selectivity. Analogs of the piperidine moiety lowered activity on PLA2G4E.
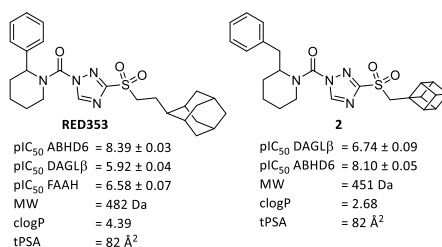
   IK015 and sulfonamide analog **WEN222** (Figure 7.1B) were selected for further biological characterization. The compounds were selective over PLA2G4B–D, NAPE-PLD and CB_1 and CB_2 receptors. In addition, **IK015** and **WEN222** showed at least 10-fold selectivity over PLAAT2–5 and more than 30-fold selectivity over most serine hydrolases characterized in mouse brain proteome, but selectivity over ABHD6 was limited (~4-fold). In Neuro-2a cells, **IK015** inhibited several enzymes at 1 μM, including ABHD6, ABHD12 and FAAH. **WEN222** was less active on most enzymes, which might indicate restricted membrane permeability. Similar to **WEN091**, the compounds showed increased activity

on FAAH in the cellular assay. Altogether, **IK015** and **WEN222** are potent and selective PLA2G4E inhibitors *in vitro* with an improved selectivity profile compared to **IK015**, but showed activity on several serine hydrolases at higher concentrations. Pyrazole urea **WEN258** was identified as structural analog with a similar off-target profile to **WEN091**, **IK015** and **WEN222** but no activity on PLA2G4E (Figure 7.1B).

To support the evidence of **WEN091**'s cellular activity on PLA2G4E, in **Chapter 5**, an activity-based probe (ABP) was developed to visualize intracellular target engagement. The design of probe **WEN175** (Figure 7.1C) was based on PLA2G4E inhibitors identified in **Chapters 2** and **4**. The triazole ureas are hypothesized to covalently modify the catalytic serine of PLA2G4E by the formation of a carbamoyl adduct, which should allow to irreversibly label active enzyme. Therefore, the carbamoylating 'staying group' of **WEN175** was equipped with an alkyne handle to which a fluorophore could be conjugated after cell lysis using copper-catalyzed alkyne-azide cycloaddition (CuAAC). This 'two-step labeling' approach circumvented cell permeability issues associated with bulky, charged fluorophores.[37,38] Probe **WEN175** was able to dose-dependently label PLA2G4E overexpressed in Neuro-2a cells, demonstrating its applicability as cellular active PLA2G4E probe. **WEN175** did not label PLA2G4E mutants in which the catalytic serine was substituted for an alanine (S412A) or the C2 domain (ΔC2) or polybasic domain (ΔPB) were removed, thereby illustrating the importance of this amino acid and motifs for the catalytic activity.[39] Importantly, pre-treatment with **WEN091** dose-dependently inhibited fluorescent labeling of PLA2G4E by **WEN175**, demonstrating cellular target engagement of **WEN091**. Despite **WEN091**'s low nanomolar IC_{50} *in vitro*, high concentrations (10 µM) were needed to obtain complete *in situ* target engagement, which is in line with the results from the targeted lipidomics experiments in **Chapter 3**. Limited cell penetration and/or high levels of competing substrates are likely to explain the need for high cellular concentrations of inhibitor **WEN091**. The tailored ABP **WEN175** is an useful chemical tool to guide the design of novel PLA2G4E inhibitors with improved cellular activity.

Caged hydrocarbons are polycyclic chemical structures with unique physicochemical properties, but they are not commonly applied in medicinal chemistry. In **Chapter 6**, nine 1,2,4-triazole ureas substituted with caged hydrocarbons were synthesized and tested as inhibitors of ABHD6, ABHD16a and DAGLα/β to investigate the effect of caged hydrocarbons on the activity of the inhibitors. All compounds inhibited their primary target with sub-micromolar IC_{50} values in an ABPP assay on mouse brain proteome. Adamant-2-ylethylene-containing ABHD6 inhibitor **RED353** and cubanemethylene-containing DAGL inhibitor **2** were further profiled in cellular assays (Figure 7.2). **2**'s activity on DAGLβ in Neuro-2a cells was lower than its activity on DAGLα *in vitro*, but **RED353** inhibited ABHD6 with pIC_{50} = 8.39 ± 0.03 and showed almost 300-fold selectivity over DAGLβ and 90-fold over FAAH. **RED353** also inhibited ABHD6-mediated fluorogenic substrate conversion in an orthogonal assay and lowered cellular 2-AG, but not anandamide, levels, outperforming

widely used ABHD6 inhibitor KT182.[40] These results confirm and extend the previous observation that ABHD6 is responsible for the tonic production of 2-AG in Neuro-2a cells.[36]

RED353

pIC$_{50}$ ABHD6 = 8.39 ± 0.03
pIC$_{50}$ DAGLβ = 5.92 ± 0.04
pIC$_{50}$ FAAH = 6.58 ± 0.07
MW = 482 Da
clogP = 4.39
tPSA = 82 Å^2

2

pIC$_{50}$ DAGLβ = 6.74 ± 0.09
pIC$_{50}$ ABHD6 = 8.10 ± 0.05
MW = 451 Da
clogP = 2.68
tPSA = 82 Å^2

Figure 7.2. Structure and properties of ABHD6 inhibitors RED353 and 2. Activity determined using gel-based ABPP on Neuro-2a cells (pIC$_{50}$ ± SEM, N = 3). Molecular weight (MW) and topological polar surface area (tPSA) calculated using ChemDraw Professional 16.0, octanol/water partition coefficient (clogP) calculated using DataWarrior 5.0.0.

Future directions

Towards improved PLA2G4E and ABHD6 inhibitors

Previously, triazole ureas have been successfully leveraged as tool compounds to study several brain serine hydrolases *in vivo*, e.g. ABHD6, ABHD16a and DAGLα/β[40–43], thereby showing the future potential for the PLA2G4E inhibitors reported in this thesis. PLA2G4E inhibitor **WEN091** showed high potency, cellular target engagement and efficacy in lowering cellular NAPE levels, but inhibited several additional serine hydrolases in Neuro-2a cells. **IK015** has an improved *in vitro* selectivity profile compared to **WEN091** and lower off-target activity in Neuro-2a cells. Further characterization of this inhibitor by investigating *in situ* target engagement, inhibition of NAPE formation and activity on other enzymes involved in NAPE metabolism (ABHD4, PLAAT1–5) will be necessary to determine whether **IK015** is a better lead candidate for *in vivo* PLA2G4E inhibition than **WEN091**. Of note, **IK015** did show inhibition of FAAH and ABHD6 at concentrations below 1 µM in a cellular setting and a relatively high topological polar surface area, which may limit brain penetration. Further optimization of the selectivity and physicochemical properties of this chemotype might, therefore, be required.

Structure-based drug design could guide the design of the next series of PLA2G4E inhibitors. Currently, there are no crystal structures available of PLA2G4E. **IK015** was, therefore, docked into a homology model of hPLA2G4E built based on the crystal structure of hPLA2G4D.[44] The predicted binding pose suggests the existence of a narrow pocket lined with hydrophobic residues, limited space around the chlorine atom and a larger pocket around the trifluoromethoxy substituent, in line with the SAR results from **Chapters 2** and **4** (Figure 7.3). The SAR suggest that substituents that create new interactions with the active site may be introduced on the *ortho* or *meta* position of the piperidyl benzyl or *para* position of the sulfonyl benzyl. These substituents might be able to increase the inhibitor's affinity for PLA2G4E and selectivity over other targets. Improving the inhibitor's

potency may potentially allow to remove heteroatoms to reduce the tPSA. One should, however, always take into consideration the effect modifications have on other physico-chemical properties, such as the lipophilicity and molecular weight. A combination of modifications might be required to obtain the optimal balance. Characterization of the pharmacokinetic properties of the inhibitors will be necessary to assess their *in vivo* applicability. Results of these studies may demand further optimization of e.g. metabolic stability, plasma protein binding or brain penetration.

The broad reactivity of triazole ureas towards serine hydrolases makes it challenging to obtain high selectivity, and many previously published triazole urea-based inhibitors have shown cross-reactivity with off-targets at elevated concentrations.[40,41,43] In addition to (adverse) off-target effects, this could lead to limited metabolic stability of the compound due to rapid enzymatic hydrolysis.[45,46] Increasing the non-covalent binding
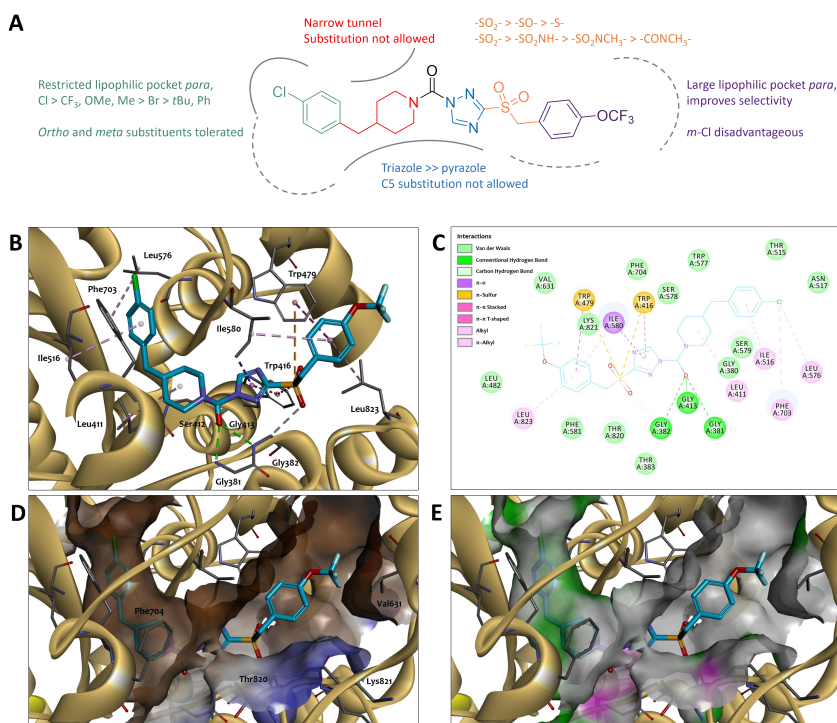
Figure 7.3. SAR overview and docking results of IK015. A) Summary of observations regarding the potency and selectivity of synthesized PLA2G4E inhibitors from the SAR studies in Chapters 2 and 4. B–E) **IK015** (cyan carbon atoms) was covalently docked to Ser[412] (bond not shown) in a homology model of hPLA2G4E (sand ribbon) based on hPLA2G4D.[44] Several amino acids interacting with **IK015** are displayed in element color. B) Highest-scored **IK015** docking pose in hPLA2G4E model with predicted enzyme–inhibitor interactions indicated. Interacting amino acids are annotated. C) 2D representation of predicted interactions of **IK015** with hPLA2G4E, corresponding to the docking pose in (B). D) Docking pose with pocket surface shown. Hydrophobic surface is indicated in brown, hydrophilic in blue. E) Docking pose with pocket surface indicating predicted hydrogen bond donating (magenta) and accepting (green) character.

affinity of the PLA2G4E inhibitors for PLA2G4E may allow to reduce the intrinsic reactivity of the urea warhead, which might lead to improved selectivity over other serine hydrolases. However, less promiscuous chemotypes might be better suited for specific PLA2G4E inhibition and high *in vivo* stability.

ABHD6 inhibitor **RED353** displayed high potency and a favorable selectivity profile in Neuro-2a cells. It showed lower activity on FAAH than KT182, but was more active on DAGLα and β. Previous studies on DAGL and ABHD6 inhibitors have shown increased selectivity for ABHD6 when polar groups were introduced on the piperidine or leaving group substituent.[40,47,48] Hence, new derivatives of **RED353** with polar substituents could be explored that might improve the ABHD6 selectivity. These can be used to study the contribution of ABHD6 to 2-AG production in other cell types and under different conditions.

PLA2G4E inhibitors may elucidate PLA2G4E and NAPE biology

PLA2G4A has been extensively exploited for the development of drugs against inflammatory conditions, and several PLA2G4A inhibitors have advanced into clinical trials.[49,50] Similarly, multiple inhibitors of enzymes involved in the endocannabinoid system have been developed to study the therapeutic potential of their targets in inflammatory pain, anxiety or metabolic syndrome.[51–54] *In vivo* active and selective PLA2G4E inhibitors would be valuable tools to study the role of PLA2G4E and NAPEs in (patho)physiological processes. They can be used to confirm the role of this enzyme in the homeostasis of NAPEs and its precursors PE and PC. Acute inhibition of PLA2G4E will allow to investigate its importance in the development of neurodegenerative diseases[8,14,24] and may illuminate the functions of NAPEs during ischemia, cytotoxicity and inflammation.[17,19,21] Furthermore, inhibition of NAPE biosynthesis may aid in clarifying the putative role of NAPEs as feeding hormones.[15,16] As PLA2G4E was reported to be localized to the endocytic machinery[7], inhibitors could be used to elucidate the function of PLA2G4E in endocytic recycling, and the role of NAPEs or other products and substrates of PLA2G4E in this process. This might also increase our knowledge on the involvement of the endocannabinoid system in intercellular signaling. In these studies, previously reported NAPE-PLD inhibitors can be used to distinguish the effects of NAPEs from that of NAEs.[54] In addition, PLAAT inhibitors can be used in conjunction with PLA2G4E inhibitors to investigate the regulation of the two pathways of NAPE biosynthesis, including their substrate preference and spatiotemporal activity.[55,56]

A PLA2G4E probe that is able to visualize endogenous activity could be used to investigate the relation between the enzymatic activity and subcellular localization of PLA2G4E. Furthermore, it may show PLA2G4E activity and localization in different cell types or brain regions. Expression of (lyso)-NAPE hydrolase ABHD4 was recently shown to be tightly regulated in developing neurons.[57] Visualization of PLA2G4E activity in neuronal

cells in different developmental states could help to elucidate which metabolites are associated with neuronal maturation, differentiation and fate.

Closing remarks

Selective and cellular active inhibitors are instrumental to study the (patho)physiological functions of enzymes. In this work, compounds **WEN091**, **WEN222**, **WEN258, IK015** and **WEN175** are presented as the first-in-class tool compounds to study the biology of PLA2G4E. These inhibitors and activity-based probe will be valuable to elucidate the importance of PLA2G4E in NAPE biosynthesis in different cells, tissues and conditions. In conjunction with previously reported inhibitors of PLAAT1–5 and NAPE-PLD, these compounds can be used to study the functionalities and roles of NAPEs in homeostasis and disease. The chemical tools developed in this thesis may help to uncover new therapeutic possibilities to treat conditions involving neurodegeneration, inflammation or feeding.

Acknowledgements

Experimental procedures

Computational chemistry

The homology structure model of human PLA2G4E was generated from the X-ray structure of hPLA2G4D (5IXC[44], obtained from The Protein Data Bank), which shared 47% sequence identity with hPLA2G4E, using SWISS-MODEL. The obtained structure was pre-processed with Schrödinger Protein Preparation Wizard using default parameters. **IK015** was pre-processed with Schrödinger LigPrep using default parameters. **IK015** was subsequently docked to the PLA2G4E model using CovDock, selecting Ser[412] as the reactive residue performing nucleophilic attack on a double bond in thorough sampling mode. Docking results were visually analyzed and images created in BIOVIA Discovery Studio 2016, during which the covalent bond between the protein and ligand was removed for practical purposes.

References

1. Coulon, D., Faure, L., Salmon, M., Wattelet, V. & Bessoule, J. J. Occurrence, biosynthesis and functions of *N*-acylphosphatidylethanolamines (NAPE): Not just precursors of *N*-acylethanolamines (NAE). *Biochimie* **94**, 75–85 (2012).

2. Wellner, N., Diep, T. A., Janfelt, C. & Hansen, H. S. *N*-acylation of phosphatidylethanolamine and its biological functions in mammals. *Biochim. Biophys. Acta - Mol. Cell Biol. Lipids* **1831**, 652–662 (2013).

3. Ogura, Y., Parsons, W. H., Kamat, S. S. & Cravatt, B. F. A calcium-dependent acyltransferase that produces *N*-Acyl phosphatidylethanolamines. *Nat. Chem. Biol.* **12**, 669–671 (2016).

4. Hussain, Z. *et al.* Phosphatidylserine-stimulated production of *N*-acyl-phosphatidylethanol-amines by Ca^{2+}-dependent *N*-acyltransferase. *Biochim. Biophys. Acta - Mol. Cell Biol. Lipids* **1863**, 493–502 (2018).

5. Leslie, C. C. Cytosolic phospholipase A_2: Physiological function and role in disease. *J. Lipid Res.* **56**, 1386–1402 (2015).

6. Ghosh, M., Tucker, D. E., Burchett, S. A. & Leslie, C. C. Properties of the Group IV phospholipase A_2 family. *Prog. Lipid Res.* **45**, 487–510 (2006).

7. Capestrano, M. *et al.* Cytosolic phospholipase $A_2\varepsilon$ drives recycling through the clathrin-independent endocytic route. *J. Cell Sci.* **127**, 977–993 (2014).

8. Pérez-González, M. *et al.* PLA2G4E, a candidate gene for resilience in Alzheimer's disease and a new target for dementia treatment. *Prog. Neurobiol.* **191**, (2020).

9. Morimoto, Y. *et al.* Whole-exome sequencing and gene-based rare variant association tests suggest that PLA2G4E might be a risk gene for panic disorder. *Transl. Psychiatry* **8**, (2018).

10. Lee, Y. C., Zheng, Y. O., Taraschi, T. F. & Janes, N. Hydrophobic alkyl headgroups strongly promote membrane curvature and violate the headgroup volume correlation due to 'headgroup' insertion. *Biochemistry* **35**, 3677–3684 (1996).

11. Domingo, J. C., Mora, M. & de Madariaga, M. A. The influence of *N*-acyl chain length on the phase behaviour of natural and synthetic *N*-acylethanolamine phospholipids. *Chem. Phys. Lipids* **75**, 15–25 (1995).

12. Shangguan, T., Pak, C. C., Ali, S., Janoff, A. S. & Meers, P. Cation-dependent fusogenicity of an *N*-acyl phosphatidylethanolamine. *Biochim. Biophys. Acta* **1368**, 171–183 (1998).

13. Mora, M., Mir, F., Madariaga, M. A. de & Sagrista, M. L. Aggregation and fusion of vesicles composed of *N*-palmitoyl derivatives of membrane phospholipids. *Lipids* **35**, 513–524 (2000).

14. Palese, F., Pontis, S., Realini, N. & Piomelli, D. NAPE-specific phospholipase D regulates LRRK2 association with neuronal membranes. in *Advances in Pharmacology* **90**, 217–238 (Academic Press Inc., 2021).

15. Wellner, N. *et al.* Studies on the anorectic effect of *N*-acylphosphatidylethanolamine and phosphatidylethanolamine in mice. *Biochim. Biophys. Acta - Mol. Cell Biol. Lipids* **1811**, 508–512 (2011).

16. Gillum, M. P. *et al.* *N*-acylphosphatidylethanolamine, a Gut-Derived Circulating Factor Induced by Fat Ingestion, Inhibits Food Intake. *Cell* **135**, 813–824 (2008).

17. Epps, D. E., Natarajan, V., Schmid, P. C. & Schmid, H. H. O. Accumulation of *N*-acylethanolamine glycerophospholipids in infarcted myocardium. *Biochim. Biophys. Acta - Lipids Lipid Metab.* **618**, 420–430 (1980).

18. Hansen, H. H., Hansen, S. H., Schousboe, A. & Hansen, H. S. Determination of the phospholipid precursor of anandamide and other *N*-acylethanolamine phospholipids before and after sodium azide-induced toxicity in cultured neocortical neurons. *J. Neurochem.* **75**, 861–871 (2000).

19. Kondo, S. *et al.* Accumulation of various *N*-acylethanolamines including *N*-arachidonoylethanol-amine (anandamide) in cadmium chloride-administered rat testis. *Arch. Biochem. Biophys.* **354**, 303–310 (1998).

20. Hansen, H. S., Lauritzen, L., Strand, A. M., Moesgaard, B. & Frandsen, A. Glutamate stimulates the formation of *N*-acylphosphatidylethanolamine and *N*-acylphosphatidylethanolamine in cortical neurons in culture. *Biochim. Biophys. Acta - Lipids Lipid Metab.* **1258**, 303–308 (1995).

21. Palese, F., Pontis, S., Realini, N. & Piomelli, D. A protective role for *N*-acylphosphatidylethanol-amine phospholipase D in 6-OHDA-induced neurodegeneration. *Sci. Rep.* **9**, 1–16 (2019).

22. Basit, A., Pontis, S., Piomelli, D. & Armirotti, A. Ion mobility mass spectrometry enhances low-abundance species detection in untargeted lipidomics. *Metabolomics* **12**, 1–10 (2016).

23. Uyama, T. *et al.* Generation of *N*-acylphosphatidylethanolamine by members of the phospholipase A/acyltransferase (PLA/AT) family. *J. Biol. Chem.* **287**, 31905–31919 (2012).

24. Vaz, F. M. *et al.* Mutations in PCYT2 disrupt etherlipid biosynthesis and cause a complex hereditary spastic paraplegia. *Brain* **142**, 3382–3397 (2019).

25. Ross, B. M., Mamalias, N., Moszczynska, A., Rajput, A. H. & Kish, S. J. Elevated activity of phospholipid biosynthetic enzymes in substantia nigra of patients with Parkinson's disease. *Neuroscience* **102**, 899–904 (2001).

26. Wang, S. *et al.* Phosphatidylethanolamine deficiency disrupts α-synuclein homeostasis in yeast and worm models of Parkinson disease. *Proc. Natl. Acad. Sci.* **111**, E3976–E3985 (2014).

27. Hussain, Z., Uyama, T., Tsuboi, K. & Ueda, N. Mammalian enzymes responsible for the biosynthesis of *N*-acylethanolamines. *Biochim. Biophys. Acta - Mol. Cell Biol. Lipids* **1862**, 1546–1561 (2017).

28. Fu, J., Kim, J., Oveisi, F., Astarita, G. & Piomelli, D. Targeted enhancement of oleoylethanolamide production in proximal small intestine induces across-meal satiety in rats. *Am. J. Physiol. - Regul. Integr. Comp. Physiol.* **295**, 45–50 (2008).

29. Provensi, G. *et al.* Satiety factor oleoylethanolamide recruits the brain histaminergic system to inhibit food intake. *Proc. Natl. Acad. Sci.* **111**, 11527–11532 (2014).

30. González-Aparicio, R. & Moratalla, R. Oleoylethanolamide reduces L-DOPA-induced dyskinesia via TRPV1 receptor in a mouse model of Parkinson's disease. *Neurobiol. Dis.* **62**, 416–425 (2014).

31. Hohmann, A. G. *et al.* An endocannabinoid mechanism for stress-induced analgesia. *Nature* **435**, 1108–1112 (2005).

32. Lutz, B., Marsicano, G., Maldonado, R. & Hillard, C. J. The endocannabinoid system in guarding against fear, anxiety and stress. *Nat. Rev. Neurosci.* **16**, 705–718 (2015).

33. Walter, L. & Stella, N. Cannabinoids and neuroinflammation. *Br. J. Pharmacol.* **141**, 775–785 (2004).

34. Meijerink, J. *et al.* Inhibition of COX-2-mediated eicosanoid production plays a major role in the anti-inflammatory effects of the endocannabinoid *N*-docosahexaenoylethanolamine (DHEA) in macrophages. *Br. J. Pharmacol.* **172**, 24–37 (2015).

35. Zhou, J. Development of a PLA2G4E Assay and Subsequent Application in Hit Identification. *Inhibitor Discovery of Phospholipase and N-Acyltransferase* (Leiden University, 2020).

36. van Esbroeck, A. C. M. *et al.* Identification of α,β-Hydrolase Domain Containing Protein 6 as a Diacylglycerol Lipase in Neuro-2a Cells. *Front. Mol. Neurosci.* **12**, (2019).

37. Speers, A. E., Adam, G. C. & Cravatt, B. F. Activity-Based Protein Profiling *in Vivo* Using a Copper(I)-Catalyzed Azide-Alkyne [3 + 2] Cycloaddition. *J. Am. Chem. Soc.* **125**, 4686–4687 (2003).

38. Gillet, L. C. J. *et al.* In-cell selectivity profiling of serine protease inhibitors by activity-based proteomics. *Mol. Cell. Proteomics* **7**, 1241–1253 (2008).

39. Binte Mustafiz, S. S. *et al.* The role of intracellular anionic phospholipids in the production of *N*-acyl-phosphatidylethanolamines by cytosolic phospholipase A$_2$ε. *J. Biochem.* **165**, 343–352 (2019).

40. Hsu, K. L. *et al.* Discovery and optimization of piperidyl-1,2,3-triazole ureas as potent, selective, and in vivo-active inhibitors of α/β-hydrolase domain containing 6 (ABHD6). *J. Med. Chem.* **56**, 8270–8279 (2013).

41. Deng, H. *et al.* Triazole Ureas Act as Diacylglycerol Lipase Inhibitors and Prevent Fasting-Induced Refeeding. *J. Med. Chem.* **60**, 428–440 (2017).

42. Hsu, K. L. *et al.* Development and optimization of piperidyl-1,2,3-triazole ureas as selective chemical probes of endocannabinoid biosynthesis. *J. Med. Chem.* **56**, 8257–8269 (2013).

43. Janssen, F. J. Discovery of 1,2,4-triazole sulfonamide ureas as *in vivo* active α/β hydrolase domain type 16A inhibitors. *Discovery of novel inhibitors to investigate diacylglycerol lipases and α/β hydrolase domain 16A* (Leiden University, 2016).

44. Wang, H. *et al.* Structure of Human GIVD Cytosolic Phospholipase A$_2$ Reveals Insights into Substrate Recognition. *J. Mol. Biol.* **428**, 2769–2779 (2016).

45. Kaur, G. *et al.* Synthesis, structure–activity relationship, and p210bcr-abl protein tyrosine kinase activity of novel AG 957 analogs. *Bioorg. Med. Chem.* **13**, 1749–1761 (2005).

46. Gehringer, M. & Laufer, S. A. Emerging and Re-Emerging Warheads for Targeted Covalent Inhibitors: Applications in Medicinal Chemistry and Chemical Biology. *Journal of Medicinal Chemistry* **62**, 5673–5724 (2019).

47. Deng, H. *et al.* Chiral disubstituted piperidinyl ureas: a class of dual diacylglycerol lipase-α and ABHD6 inhibitors. *Medchemcomm* **8**, 982–988 (2017).

48. Janssen, A. P. A. Hit-to-Lead Optimization of Triazole Sulfonamide DAGL-α inhibitors. *Inhibitor Selectivity: Profiling and Prediction* (Leiden University, 2019).

49. Duvernay, M. T., Matafonov, A., Lindsley, C. W. & Hamm, H. E. Platelet Lipidomic Profiling: Novel Insight into Cytosolic Phospholipase A$_2$α Activity and Its Role in Human Platelet Activation. *Biochemistry* **54**, 5578–5588 (2015).

50. Lee, K. L. *et al.* Discovery of ecopladib, an indole inhibitor of cytosolic phospholipase A$_2$α. *J. Med. Chem.* **50**, 1380–1400 (2007).

51. Ogasawara, D. *et al.* Selective blockade of the lyso-PS lipase ABHD12 stimulates immune responses *in vivo*. *Nat. Chem. Biol.* **14**, 1099–1108 (2018).

52. Johnson, D. S. *et al.* Discovery of PF-04457845: A Highly Potent, Orally Bioavailable, and Selective Urea FAAH Inhibitor. *Chem. Lett* **2**, 91–96 (2011).

53. Baggelaar, M. P. *et al.* Highly Selective, Reversible Inhibitor Identified by Comparative Chemoproteomics Modulates Diacylglycerol Lipase Activity in Neurons. *J. Am. Chem. Soc.* **137**, 8851–8857 (2015).

54. Mock, E. D. *et al.* Discovery of a NAPE-PLD inhibitor that modulates emotional behavior in mice. *Nat. Chem. Biol.* **16**, 667–675 (2020).

55. Zhou, J. *et al.* Activity-Based Protein Profiling Identifies α-Ketoamides as Inhibitors for Phospholipase A$_2$ Group XVI. *ACS Chem. Biol.* **14**, 164–169 (2019).

56. Zhou, J. *et al.* Structure-Activity Relationship Studies of α-Ketoamides as Inhibitors of the Phospholipase A and Acyltransferase Enzyme Family. *J. Med. Chem.* **63**, 9340–9359 (2020).

57.   László, Z. I. *et al.* ABHD4-dependent developmental anoikis safeguards the embryonic brain. *Nat. Commun.* **11**, 1–16 (2020).